

# Supplementary: Effect of Lipid Head Group Interactions in Membrane Properties and Membrane-Induced Cationic $\beta$ -Hairpin Folding<sup>†</sup>

Sai J Ganesan,<sup>a,c</sup> Hongcheng Xu,<sup>b,c</sup> and Silvina Matysiak<sup>\*d‡</sup>

---

<sup>0a</sup> Department of Bioengineering, University of Maryland, College Park, Maryland, USA.

<sup>0b</sup> Biophysics Program, University of Maryland, College Park, Maryland, USA.

<sup>0d</sup> Department of Bioengineering and Biophysics Program, University of Maryland, College Park, Maryland, USA. Tel: 301 405 0313; E-mail: matysiak@umd.edu

<sup>0c</sup> S. J. Ganesan and H. C. Xu contributed equally to this work.

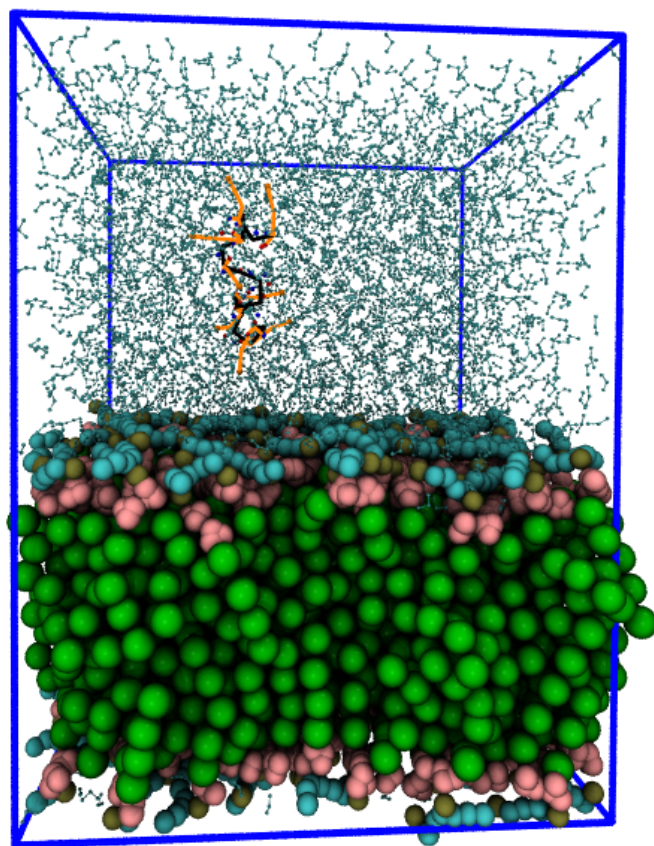


Fig. S1: Bilayer peptide system setup. Peptide is placed 5 nm away from the bilayer.

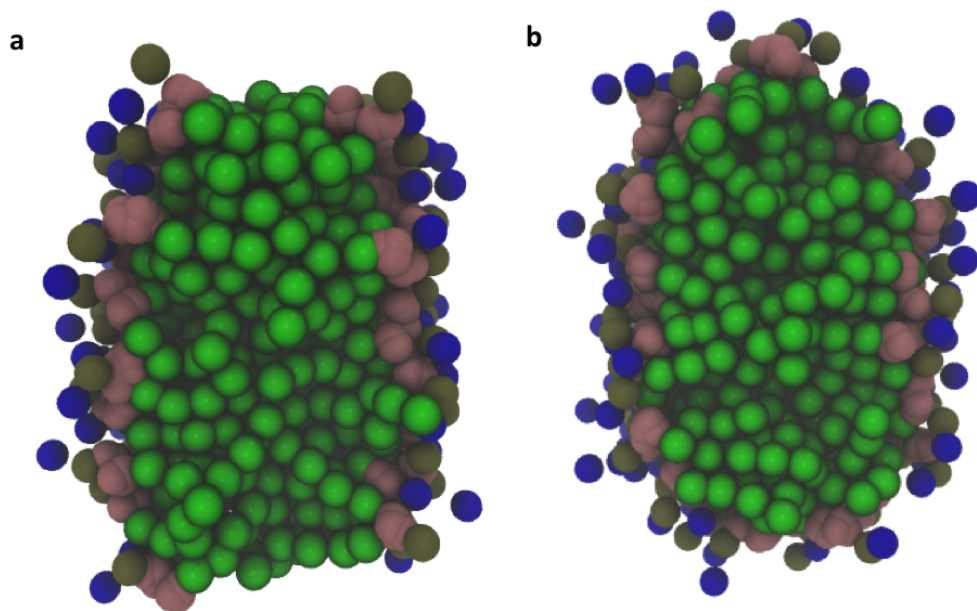


Fig. S2: Line tension ribbon structure. Phosphates are represented in brown, ester groups in pink, choline groups in blue, alkyl groups in green.

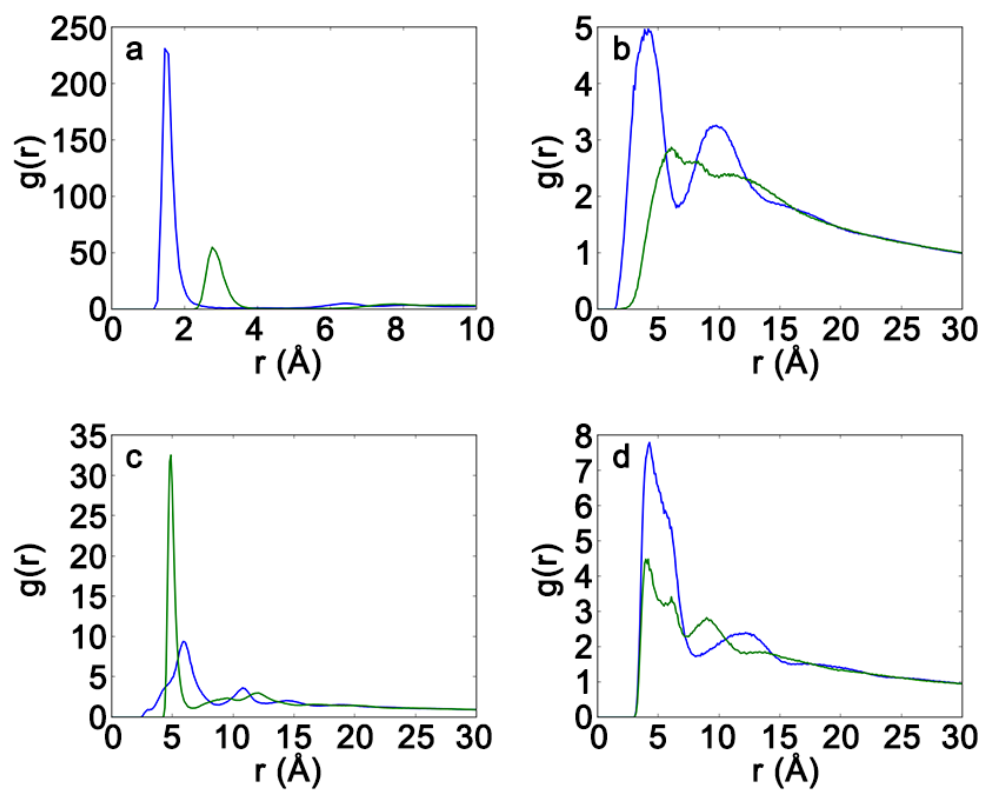


Fig. S3: Radial distribution functions for serine-involved (a-b) and ion-involved (c-d) electrostatic interaction pairs. (a) CNP-CNM (blue) and CNP-PO4 (green), (b) CNP-G1M (blue) and CNP-G2M (green), (c) ION-CNM (blue) and ION-PO4 (green), (d) ION-G1M (blue) and ION-G2M (green).

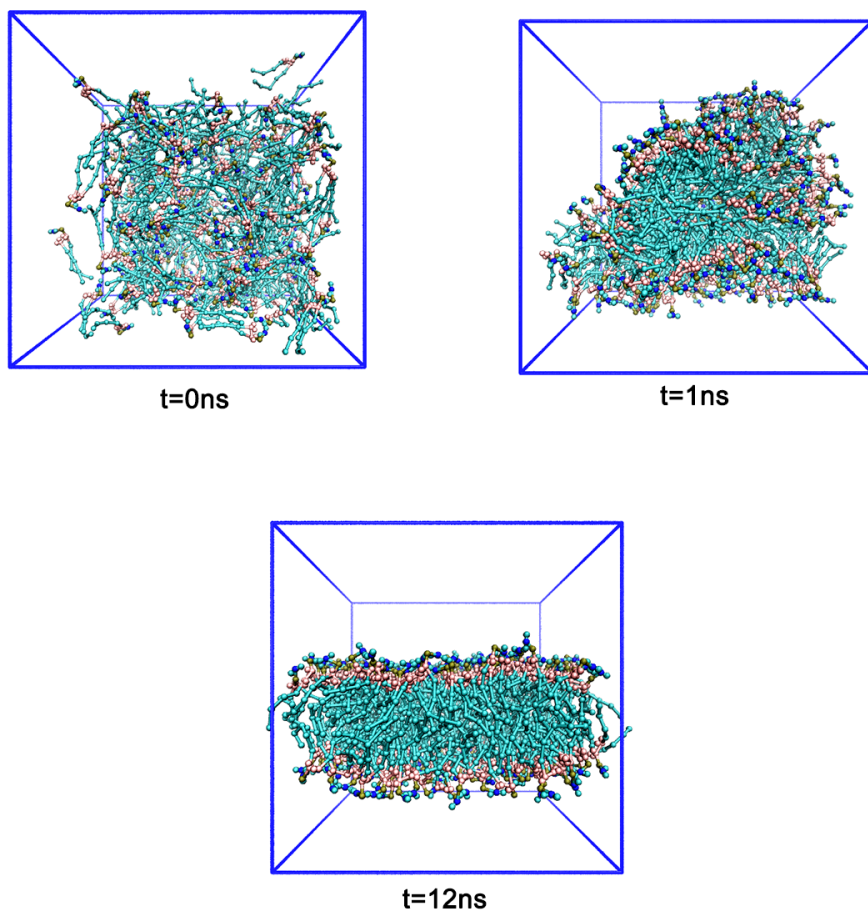


Fig. S4: Time evolution of bilayer self assembly using pCG (polarizable coarse-grained) POPS. Phosphates are represented in brown, ester groups in pink, serine groups in blue, other groups in cyan.

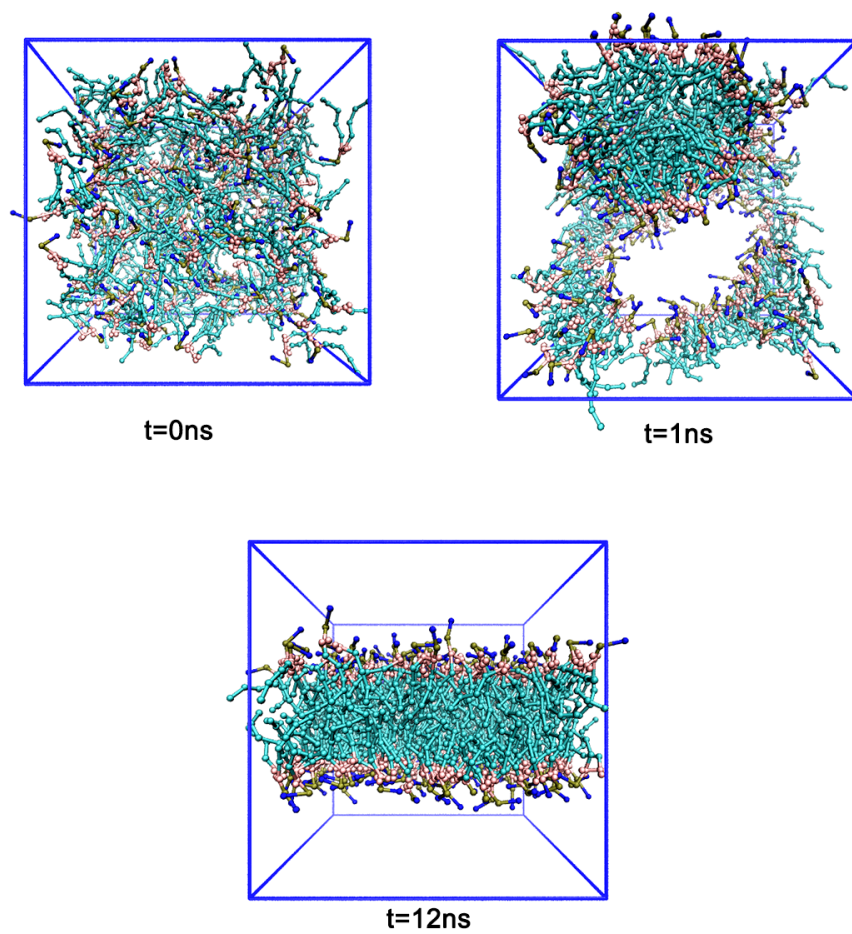


Fig. S5: Time evolution of bilayer self assembly using pCG POPC. Phosphate beads are represented in brown, ester groups in pink, choline groups are in blue, other groups in POPC in cyan.

Table S1: Bilayer thickness in different systems evaluated over last 100 ns data

System	Bilayer thickness (Å)	Standard error
POPC (MARTINI)	42.7	0.04
POPC + 1M NaCl (MARTINI)	43.7	0.03
POPS (MARTINI)	41.6	0.04
POPS + 1M NaCl (MARTINI)	43.1	0.03
POPC (pCG)	44.2	0.03
POPC + 1M NaCl (pCG)	44.9	0.03
POPS (pCG)	43.7	0.03
POPS + 1M NaCl (pCG)	44.4	0.03

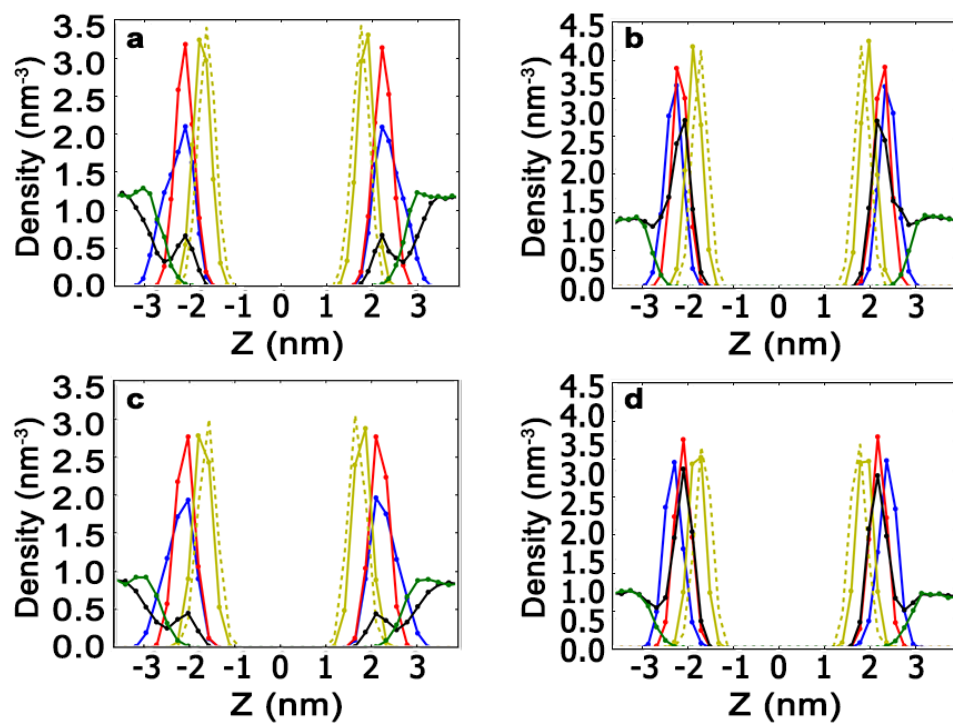


Fig. S6: Density profiles of lipid bilayer systems with 1M NaCl. Solid brown: GL1; dashed brown: GL2; red: PO4; blue: NC3/CNO; black: Na<sup>+</sup>; green: Cl<sup>-</sup>. Density distribution of (a) POPC with 1M NaCl from pCG data, (b) POPS with 1M NaCl from pCG data, (c) POPC with 1M NaCl from MARTINI data, (d) POPS with 1M NaCl from MARTINI data.

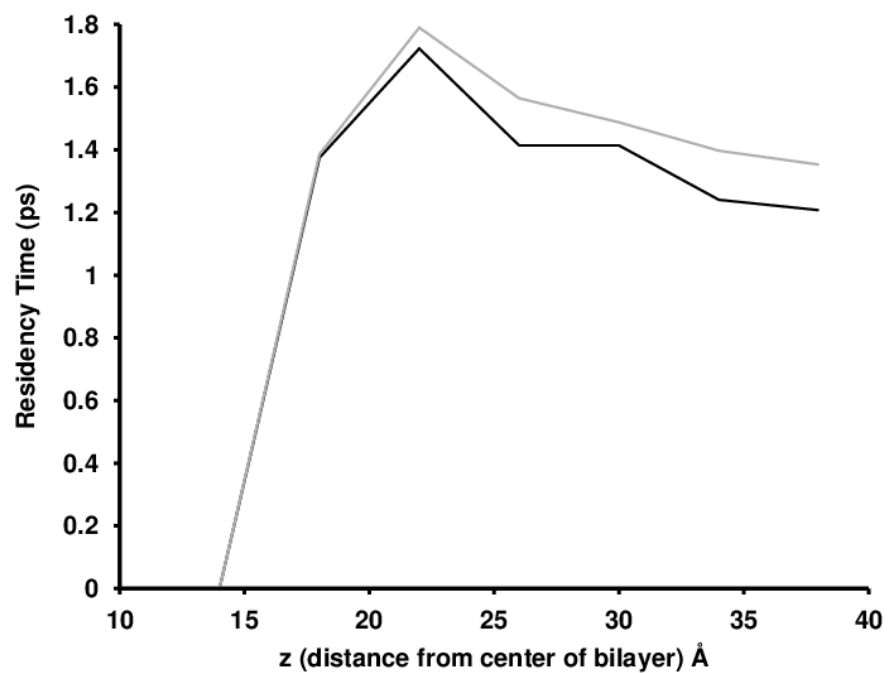


Fig. S7: Residency time ( $\tau$ ), as a function of distance from the bilayer center for counter ions in pCG POPS system (black curve) and extra added ions (gray curve).

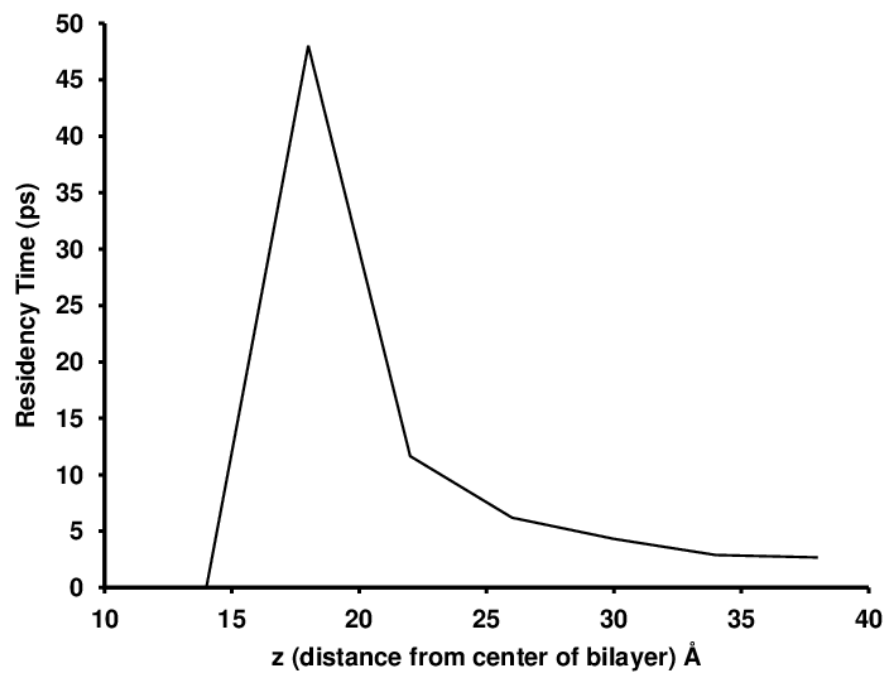


Fig. S8: Residency time ( $\tau$ ), as a function of distance from the bilayer center for ions in all-atom POPS system.



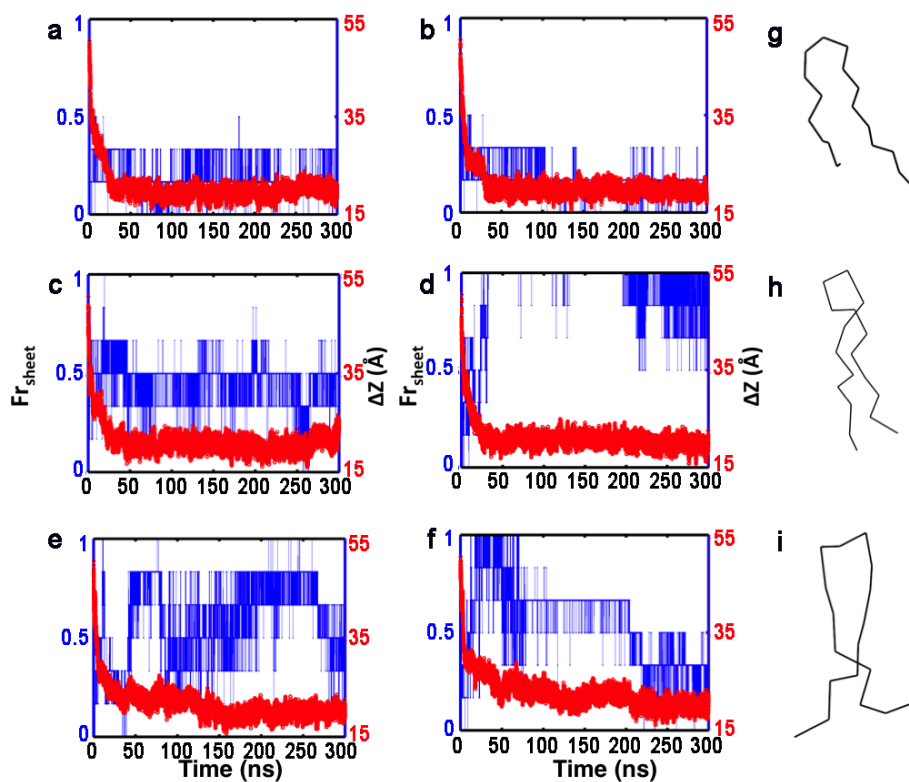


Fig. S10: Time evolution of sheet pair fraction of the peptide ( $Fr_{sheet}$ ) in blue and center of mass (com) distance of the peptide from the bilayer in red, for system with pCG POPs. a-f represents individual trials, and g, h and i are final conformations of trials depicted in c, d and e, respectively.

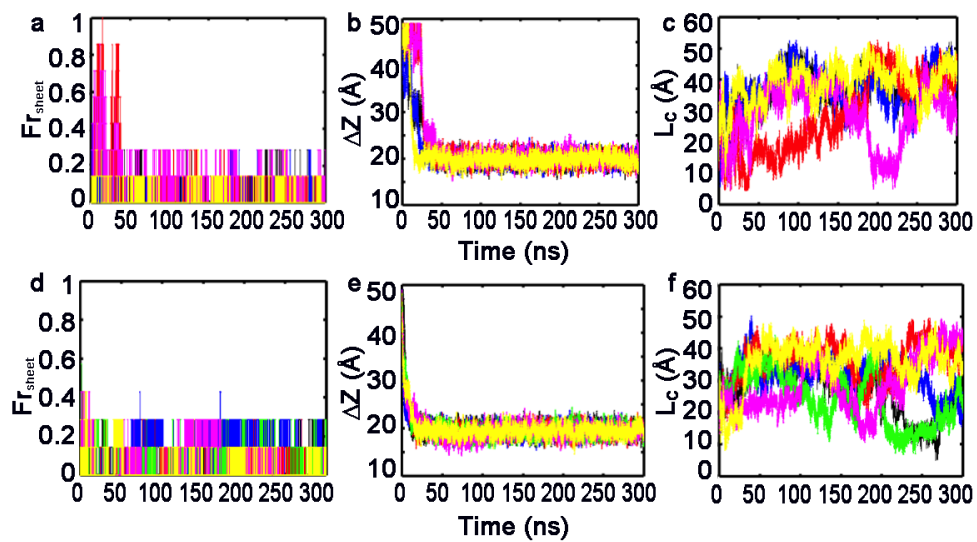


Fig. S11: Time evolution of (a and d) sheet pair fraction of the peptide ( $Fr_{sheet}$ ); (b and e) center of mass (com) distance of the peptide from the phosphate beads on the bilayer; (c and f) end to end distance ( $L_c$ ) of the peptide, evaluated between the first and the last backbone bead. Each color represents a single run. (a), (b) and (c) are data from our polarizable coarse-grained model for POPC bilayer (d), (e) and (f) are data using our peptide model with dipoles and a POPS bilayer without dipole particles (POPSnd).

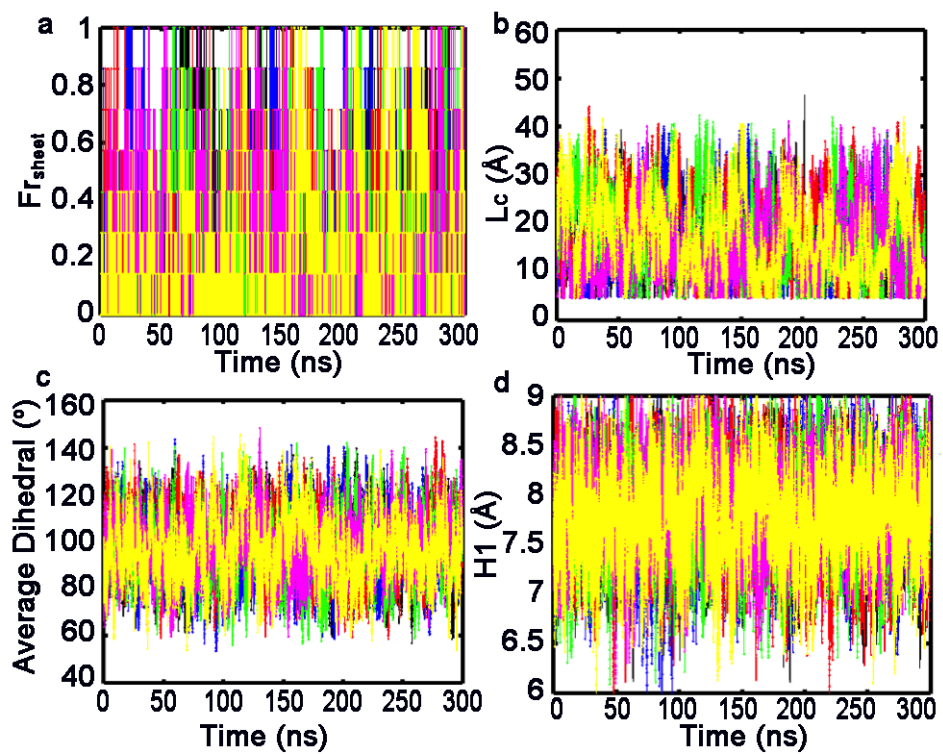


Fig. S12: Time evolution of (a) sheet fraction ( $Fr_{sheet}$ ) of the peptide in water, (b) end to end distance ( $L_c$ ), (c) average dihedral angle per frame and (d) average 1-4 backbone distances ( $H1$ ). Each color represents a single run.

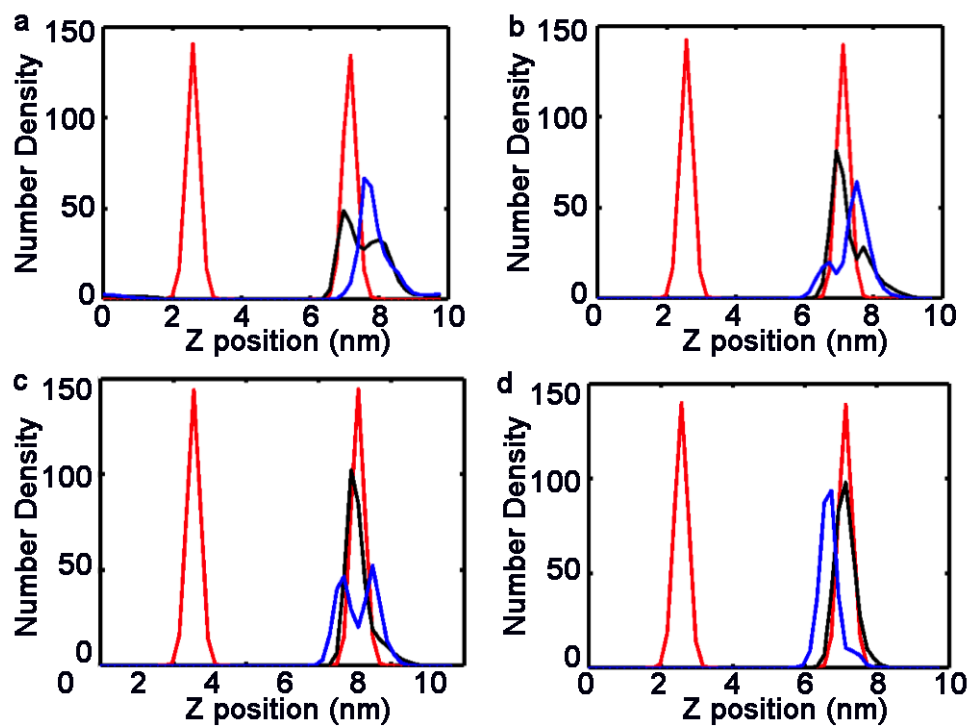


Fig. S13: Number density distribution of PO4 (red curves), lysine side chain ( $SC_{C+}$ ) (black curves) and valine side chain beads (blue curves) for POPS system, over a time period of (a) 0-25 ns, (b) 25-50 ns, (c) 50-75 ns and (d) 75-100 ns. Side chain distributions are scaled by a factor of 5 for easy comparison.

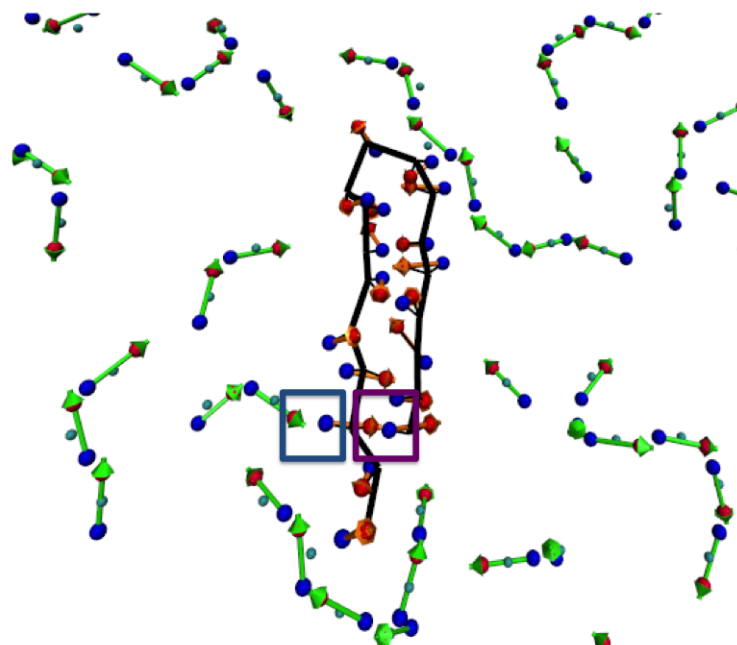


Fig. S14: Top view of a representative conformation of folded SVS-1 on POPS membrane. Peptide backbone is depicted in black, red and blue represent negatively and positively charged dummy beads. Brown vectors represent backbone dipoles and green vectors, CNO dipoles. Purple box denotes an example of dipolar connections or contacts within a peptide, that play a role in secondary structure content. Blue box denotes an example of peptide-membrane dipolar connections formed between backbone and CNO dummies.

### **Interactions between Ion and Head Groups:**

We further investigated interactions between ion and lipid head groups, to better characterize subtle changes in bilayer properties. Figure S13a shows a representative structure of a POPS lipid bound to  $\text{Na}^+$ . In this image, the  $\text{Na}^+$  ion is seen interacting with  $\text{PO}_4$ , CNO (negatively charged dummy CNM) bead and G1M dummy bead.

Sodium ions occupy the region between serine, phosphates and the ester groups, maximizing interaction with all three charged regions. This can also be seen from density plots (Figure 4d and S7b), where the sodium ions (black curve) occupy a region between CNO (blue curve) and  $\text{PO}_4$  (red curve), which lie on the same z plane, and ester groups (brown curves).

A consequence of this is a tilt in ester group vector (defined as GL1-G1M), where the negatively charged dummy, rises from the plane to interact with the sodium ion. To further quantify this effect, the angle between the ester group and its negatively charged dummy (GL1-G1M) vector with the POPS bilayer normal is measured.

In Figure S13b, the angle distribution shows two distinct peaks, accounting for the angle made by ester groups near a sodium ion, which is better aligned to the bilayer normal (peak at  $75^\circ$ ); and another, away, which is less aligned (peak at  $125^\circ$ ). For the 1M NaCl system, the GL1-G1M vector is better aligned to the bilayer normal, compared to the system with 0M NaCl. The better alignment of the GL1-G1M vector with the bilayer normal at 1M NaCl can be rationalized by the increase in population of ion bound lipids.

Figure S13c shows a representative structure of a POPC lipid bound to  $\text{Na}^+$ . In this image, the ion ( $\text{Na}^+$ ) bound to a lipid is more exposed, due to favorable interactions with phosphates. The angle between  $\text{PO}_4$ -NC3 (head groups) and the bilayer normal is depicted in Figure S13d. The  $\text{PO}_4$ -NC3 vector is better aligned with the bilayer normal with 0M NaCl (peak at  $75^\circ$ ). However, for 1M NaCl, this angle shifts (peak at  $100^\circ$ ), indicating a possible in-plane alignment of  $\text{PO}_4$ -NC3 vector, as seen in Figure S13d. This is potentially one of the reasons on why there is lesser ion penetration in POPC membranes. A study by Woolf et al. shows a similar head group tilt observed in all-atom MD simulations of POPC with 1M NaCl<sup>1</sup>.

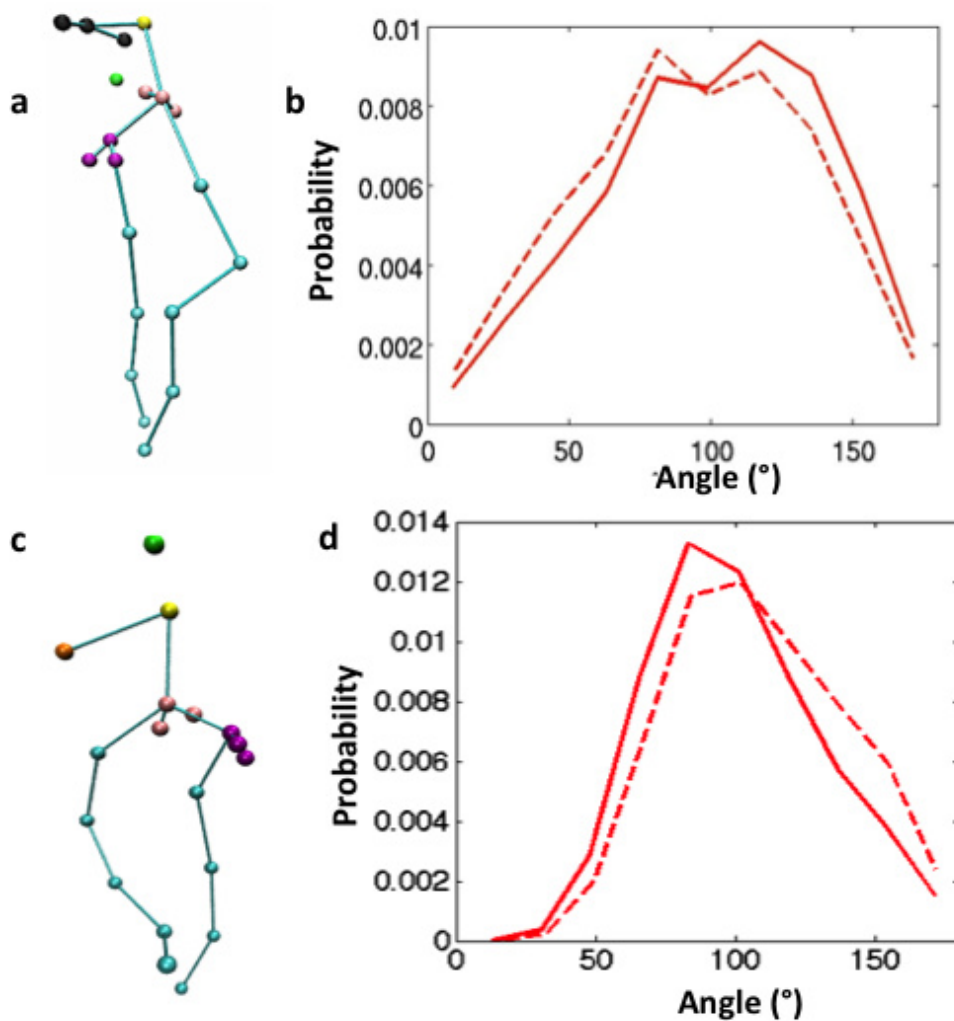


Fig. S15: (a) Representative structure of POPS lipid bound to Na<sup>+</sup>. Colors: Na<sup>+</sup> (green), CNO (black), PO4 (brown), GL1(pink), GL2(violet), alkyl (cyan) (b) Probability distribution of the angle made by the GL1-G1M vector of POPS with the bilayer normal in POPS (red). Dashed lines represent the systems with 1M NaCl and solid lines for 0M NaCl. (c) Representative structure of POPC lipid bound to Na<sup>+</sup>. Colors: Na<sup>+</sup> (green), NC3 (brown), PO4 (brown), GL1(pink), GL2(violet), alkyl (cyan). (d) Probability distribution of the angle made by the PO4-NC3 vector with bilayer normal in POPC. The dashed lines represent the systems with 1M NaCl and solid lines 0M NaCl

### Dipolar Cluster Half-Life

We have quantified the dynamics of lipid exchange (in reduced unit as lipid-exchange distance, see Methods to Calculate Dipolar Cluster Half-Life for details) between clusters (Figure S14). The lipid exchange in the POPS bilayer with 1M NaCl is more frequent than that without NaCl, because the salt screening effect destabilizes the POPS clusters by hindering the formation of CNO dipole-dipole interactions. We have also quantified the exchange half-life for the pCG POPS bilayer without NaCl (1.5 ns) and with 1M NaCl (1.0 ns, faster exchange). To get a qualitative comparison, we have shown in Figure S14 the estimated lipid exchange in pCG POPC bilayer. It should be noted that, based on the distance criteria to cluster the lipids, most POPC lipids are not grouped with any other POPC, in which case we treat those lipids as a single lipid cluster. As with the MARTINI model, there is almost no real cluster formed in either PC or PS as stated in the manuscript.

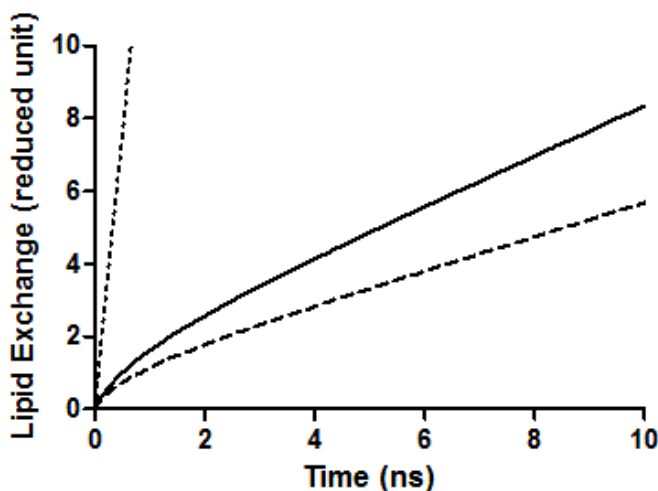


Fig. S16: Time evolution of the lipid exchange in clusters. Y axis measures the frequency of lipid exchanges in clusters by lipid-exchange distance as defined. The solid line is pCG POPS cluster with 1M NaCl, the dashed line is pCG POPS cluster without NaCl, and the dotted line is an estimate of lipid exchange in pCG POPC when POPC lipids are treated as “clusters” based on the distance criteria.

### Method to Calculate Dipolar Cluster Half-Life

One of the dynamic characteristics of lipid clusters is the half-life, which is the time required for a cluster to have half of its lipids dispersed to other clusters. To compute this half-life of clusters, we assume that lipids exchange between clusters at a fixed rate independently. A similar method has been used in a DNA evolution model (JC69)<sup>2</sup>, to characterize the mutation dynamics of DNA nitrogen base from one nucleotide base to another.

At a given time frame  $t$  in the simulation, the ensemble of all clusters present in the bilayer is denoted as a state variable  $X_t$ . Each cluster in the ensemble is indexed from 1 to total number of clusters  $n$ . We denote  $q_{ij}$  as the rate for a lipid to transfer from one cluster  $i$  to another cluster  $j$ , which is a measure of system dynamics. The matrix  $\underline{\underline{Q}} = \{q_{ij}\}$ , a probability transition matrix that characterizes the lipid-transfer rate from the  $i^{\text{th}}$  cluster in state  $X_t$  to the  $j^{\text{th}}$  cluster in state  $X_{t+\delta t}$  is defined as:

$$\underline{\underline{\mathbf{Q}}} = \{q_{ij}\} = \begin{bmatrix} -(n-1)\lambda & \lambda & \lambda & \dots & \lambda \\ \lambda & -(n-1)\lambda & \lambda & \dots & \lambda \\ \lambda & \lambda & -(n-1)\lambda & \dots & \lambda \\ \dots & \dots & \dots & \dots & \dots \\ \lambda & \lambda & \lambda & \dots & -(n-1)\lambda \end{bmatrix} \quad (1)$$

where  $i, j = 1, 2 \dots n$ , and  $\lambda$  is the infinitesimal rate for a lipid to transition from one cluster to another one. The time-dependent transition probability matrix  $\mathbf{P}$ , which denotes the probability  $p_{ij}$  for lipids in cluster  $i$  at time  $t_0$  to transfer to cluster  $j$  at time  $t_0 + t$ , is denoted below:

$$\underline{\underline{\mathbf{P}}} = \{p_{ij}\} = \begin{bmatrix} p_0 & p_1 & p_1 & \dots & p_1 \\ p_1 & p_0 & p_1 & \dots & p_1 \\ p_1 & p_1 & p_0 & \dots & p_1 \\ \dots & \dots & \dots & \dots & \dots \\ p_1 & p_1 & p_1 & \dots & p_0 \end{bmatrix} \quad (2)$$

$$p_0(t) = \frac{1}{n} + \frac{n-1}{n} e^{-n\lambda t} \quad (3)$$

$$p_1(t) = \frac{1}{n} - \frac{1}{n} e^{-n\lambda t} \quad (4)$$

$p_0(t)$  is the time-cumulative probability for a lipid to stay in the initial cluster, and  $p_1(t)$  is the time-cumulative probability for a lipid to transfer to another cluster. These probabilities are not directly computable in a simulation. However, the proportion of lipids that does not transfer to other clusters is estimated by computing from the simulation, the average ratio of number of lipids that leave the initial cluster  $N_{trans}$  and the total number of lipids  $N_{total}$  in the initial cluster:

$$(n-1)\hat{p}_1 = \left\langle \frac{N_{trans}}{N_{total}} \right\rangle. \quad (5)$$

The  $\hat{p}$  in equation (7) is referred as the  $p$ -distance, and measures how far two ensembles of clusters at different time intervals, deviate from each other. Larger the  $p$ -distance, the more lipids are transferred from a cluster when compared to the initial state. From equation (6) and (7), the estimated time-dependent lipid-transfer distance  $\hat{d}$ , defined as the product of lipid-transfer rate  $\lambda$  and time taken  $t$ , is expressed as:

$$\hat{d}(t) = \lambda t = -\frac{n-1}{n} \log\left(1 - \frac{n}{n-1} \hat{p}_1\right) \quad (6)$$

where,  $1 - \frac{n}{n-1} \hat{p}_1$  represents the proportion of lipids that transfer out of the initial cluster. The lipid-transfer rate  $\lambda$  is then computed by fitting the estimated time-dependent lipid-transfer distance  $\hat{d}(t)$ , to a linear region. From the equation (8), the half-life time of a cluster with size  $n$  is given by:

$$T_{\frac{1}{2}} = \mathbf{t}(\hat{p}_0 = 0.5) = \frac{(n-1) \log\left(2 + \frac{2}{n-2}\right)}{n\hat{\lambda}} \quad (7)$$

where  $T_{\frac{1}{2}}$  is the cluster half-life.

## References

- 1 J. N. Sachs, H. Nanda, H. I. Petrache and T. B. Woolf, *Biophys. J.*, 2004, **86**, 3772–82.
- 2 T. H. Jukes and C. R. Cantor, *Mamm. Protein Metab.*, 1969, **3**, 21–132.